Proceedings of the 2007 American Control Conference
Marriott Marquis Hotel at Times Square
New York City, USA, July 11-13, 2007

Aliasing of Resonance Phenomena in Sampled-Data Feedback Control Design: Hazards, Modeling, and a Solution

Tom Oomen, Marc van de Wal, and Okko Bosgra

Abstract— **High-performance control design for electromechanical sampled-data systems with aliased plant dynamics is investigated. Though from a theoretical viewpoint the aliasing phenomenon is automatically handled by direct sampled-data control, such an approach cannot be used in conjunction with models derived through system identification. From a practical viewpoint, aliasing is often considered as an undesirable phenomenon and a typical remedy is the increase of the sampling frequency. However, the sampling frequency is upper bounded due to physical and economical constraints and aliasing may be inevitable. Control design for plants with aliased dynamics has not received explicit attention in the literature and it is not clear how to handle this situation. In this paper, it is shown that aliased resonance phenomena can effectively be suppressed in sampled-data feedback control design without the need for increasing the sampling frequency. Furthermore, it is shown experimentally on an industrial wafer stage that ignoring aliasing during control design can have a disastrous effect on closed-loop performance. Additionally, a novel, practically feasible procedure for identification of (possibly aliased) resonance phenomena based on multirate system theory is proposed.**

I. INTRODUCTION

Industrial high-precision six degrees-of-freedom (DOFs) positioning systems are subject to increasing demands regarding speed and accuracy. An example of such a system is a wafer stage that is part of a wafer scanner. These scanners are used for the production of integrated circuits (ICs), see [15]. The market position of the wafer scanner is mainly determined by the accuracy of the produced ICs and the throughput of the machine [8]. The former translates into typical requirements of the wafer stage position accuracy in the order of nanometers, whereas the latter translates into high scan velocities and accelerations of approximately $0.5\ \mathrm{m/s}$ and $10\ \mathrm{m/s^2}$, respectively. Besides a nearly perfect electromechanical design, a state-of-the-art control system is indispensable for the satisfaction of these ever-increasing demands.

The controller for a high-performance electromechanical application is typically implemented in a digital environment because of high flexibility and relatively low cost. The sampling frequency is generally fixed because of economical and computational reasons. Hence, the controlled system is a sampled-data (SD) system, where performance is evaluated in continuous time (CT) and the controller operates in discrete time (DT). A key phenomenon in SD systems is *aliasing* [12]. Aliasing arises when signal components from high frequency bands appear in the primary frequency band after sampling. Though aliasing arises at a signal level, if causal digital-analog converters are present, then plant dynamics are also subject to aliasing [3]. Aliasing can be reduced by using causal anti-aliasing filters, however, it can never be eliminated completely.

Roughly speaking, there are three approaches to design a DT controller for an SD system:

1) direct SD control design [2], [20], [3],
2) CT design with *a posteriori* controller discretization [5],
3) plant discretization and subsequent DT design [5].

Direct SD control design handles the aliasing phenomenon automatically and is formally the ideal approach for high-performance control. In Approach 2 the aliasing phenomena are completely neglected, which generally results in performance degradation or even closed-loop instability. In Approach 3, the aliasing phenomenon is inherent to the method and is dealt with implicitly. However, if such a DT approach is employed, no guarantees can be given regarding the resulting intersample response. Indeed, in [9] it is shown that if exogenous *disturbances* are aliased, the intersample response may become arbitrarily poor if a DT approach is employed. Additionally, contrary to system poles, sampling zeros have been given considerable attention [1] and it is well-known that cancelation of sampling zeros leads to poor intersample behavior [19].

The first step in the control design for a realistic system is modeling. For high-performance electromechanical motion systems, flexible dynamics are particularly important to incorporate in the model, since these limit the achievable performance and can endanger closed-loop stability [14], [4]. Accurate models for control of these flexible dynamics are obtained through system identification (SI) [7], where DT measurements from the real system are used. Though the sampling frequencies of the measurements can be rather high, the resulting model necessarily evolves in DT. Since in direct SD control it is assumed that a CT plant model is available, SI and direct SD control cannot be combined directly in a control design cycle. Combining SI with direct SD control has been addressed in [10], [9], where resort is taken to a multirate (MR) solution [16] to arrive at a practically feasible design framework.

The aliasing of plant dynamics in identification and subsequent control design has not been addressed explicitly in the literature from an SD perspective. The main contribution of this paper is a thorough analysis of such aliased plant dynamics and its implications for control design. New results,

T. Oomen and O. Bosgra are with the Eindhoven University of Technology, Eindhoven, The Netherlands, t.a.e.oomen@tue.nl, o.h.bosgra@tue.nl.

M. van de Wal is with Philips Applied Technologies, Eindhoven, The Netherlands, m.m.j.van.de.wal@philips.com.

1-4244-0989-6/07/$25.00 ©2007 IEEE.

both theoretical and experimental, show that these aliased plant dynamics can effectively be dealt with from an SD perspective. Additionally, a novel approach is presented to identify flexible dynamics of an LTI system.

The outline of this paper is as follows. In Section II, experimental modeling of mechanical systems is investigated and the problem formulation is stated. In Section III, a design framework for SD systems is reviewed, which provides a basis for the subsequent sections. In Section IV, an identification procedure for the accurate modeling of flexible dynamics is presented. Then, in Section V, suppression of aliased resonance phenomena is addressed. Finally, conclusions and open issues are given in Section VI. To facilitate the exposition, the results are mainly discussed for the SISO case.

II. EXPERIMENTAL MODELING OF SD SYSTEMS

In this section, the class of electromechanical systems under consideration is defined. Then, experimental modeling of flexible systems is considered (Section II-B) and its implications for SD control (Section II-C). The problem formulation is stated in Section II-D.

A. System description

The considered systems are electromechanical motion systems, which are mechanical structures that are electromagnetically actuated and the output is a position or a derivative thereof. These systems have n_{rb} rigid-body modes, corresponding to the motion DOFs. Furthermore, parasitic dynamics are present in any realistic system, *e.g.*, due to mechanical flexibilities, actuator dynamics, or sensor dynamics. By an almost perfect construction, the system dynamics are almost linear.

Assumption 1 *The true, unknown system P_c evolves in CT and is assumed to be LTI and has a state-space realization*

$$P_c = \left[\begin{array}{c|c} A_c^p & B_c^p \\ \hline C_c^p & D_c^p \end{array}\right] = \left[\begin{array}{cc|c} A_{rb} & 0 & B_{rb} \\ 0 & A_f & B_f \\ \hline C_{rb} & C_f & 0 \end{array}\right], \qquad (1)$$

where $\Re(\lambda_i(A_f)) < 0$, $A_{rb} \in \mathbb{R}^{2n_{rb}\times 2n_{rb}}$, $\lambda_i(A_{rb}) = 0$, $i = 1,\ldots,2n_{rb}$, (A_{rb}, B_{rb}) controllable, and (A_{rb}, C_{rb}) observable.

The system representation (1) is standard [6], where A_f represents the possibly infinitely many, unknown, and asymptotically stable modes in addition to the unstable, observable, and controllable rigid body dynamics represented by A_{rb}.

B. Experimental modeling of flexible systems

For electromechanical motion systems, SI techniques are indispensable to obtain an accurate model for control design. SI should be performed in closed-loop, since the open-loop system (1) is unstable. Then, the data used for SI are typically extracted from the DT control loop, *e.g.*, the plant input ν_p, plant output ψ_p, and reference ρ as depicted in Fig. 1.

The ideal sampler and ZOH are defined next.

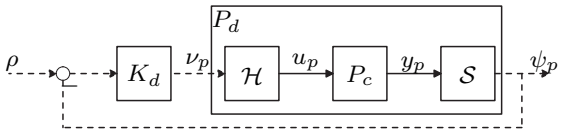

Fig. 1. Setup for experimental modeling.

Definition 2 (Sampler) *The sampling operation $\mathcal{S}$, see Fig. 1, is defined by*

$$\psi_p[k] = \mathcal{S}(y_p)[k] := y_p(kh), \qquad (2)$$

where $h := \frac{2\pi}{\omega_s} = \frac{1}{f_s}$ denotes the sampling time and $\omega_s \in \mathbb{R}$ is the angular sampling frequency, $\omega_s > 0$. The Fourier transforms $\Psi_p(e^{j\omega h})$ and $Y_p(j\omega)$ of $\psi_p[k]$ and $y_p(t)$, respectively, are related by [5]

$$\Psi_p(e^{j\omega h}) = \frac{1}{h}\sum_{k=-\infty}^{\infty} Y_p(j\omega - jl\omega_s). \qquad (3)$$

It is clear from (3) that $\Psi_p(e^{j\omega h})$ is periodic with period ω_s. Quantization effects are not addressed in (2). Aliasing is the phenomenon where the Fourier transform of $Y_p(j\omega)$ contains frequency components $|\omega| > \frac{\omega_s}{2}$ that contribute to the Fourier transform $\Psi_p(e^{j\omega h})$.

Definition 3 (ZOH) *The ZOH reconstructor $\mathcal{H}$, see Fig. 1, is defined by*

$$u_p(kh+\tau) = \mathcal{H}(\nu_p)[k] := \nu_p[k], \quad \tau \in [0, h). \qquad (4)$$

The Fourier transforms $U_p(j\omega)$ and $N_p(e^{j\omega h})$ of u_p and ν_p, respectively, are related by [5]

$$U_p(j\omega) = \frac{1 - e^{-j\omega h}}{j\omega} N_p(e^{j\omega h}). \qquad (5)$$

The ZOH-discretization P_d of the CT system P_c, see Fig. 1, is now obtained by $P_d := \mathcal{S}P_c\mathcal{H}$. Aliasing of plant dynamics can be explained as follows. If $\nu_p \neq 0$, then u_p contains signal components outside the primary frequency band, *i.e.*, for $\omega > |\frac{\omega_s}{2}|$, see (5). The CT plant P_c is thus excited at frequencies $|\omega| > \frac{\omega_s}{2}$. Subsequently, since P_c is LTI, the same frequency components are present in the plant output y_p. These high-frequent components in y_p are observed in the primary frequency band $|\omega| < \frac{\omega_s}{2}$ through (3). Thus, if P_c has a large amplification at high frequencies, *e.g.*, due to a resonance frequency, then this will be observed at lower frequencies. Note that the discussion on plant zeros in SD systems is more involved [1] and is not addressed here.

Standard SI techniques, either in the time domain [7] or in the frequency domain [11] can be applied to obtain an unique model P_d for a suitably chosen criterion. Though the estimation is performed in closed-loop, it is possible to obtain an unbiased estimate of the plant [18]. The aliasing of disturbances [9] during identification does not introduce bias errors: the effect of these disturbances is averaged out if there is no correlation with the reference signals. Contrary to the unbiased and unique identification of P_d, it is impossible to uniquely determine a model of P_c.

Proposition 4 *Given sampled measurements of the CT system P_c, see Fig. 1 and Assumption 1, it is impossible to uniquely determine a model of the CT plant P_c.*

Lemma 5 *Given a CT model P_c with state-space realization (A^p, B^p, C^p, D^p), the ZOH discretization P_d is given by*

$$P_d = \left[\begin{array}{c|c} A_d^p & B_d^p \\ \hline C_d^p & D_d^p \end{array}\right] = \left[\begin{array}{c|c} e^{A_c^p h} & \int_0^h e^{\tau A_c^p} d\tau B_c^p \\ \hline C_c^p & D_c^p \end{array}\right], \quad (6)$$

Proof: See [3]. ■

Proof: (of Proposition 4) The modeling of a CT system from DT measurements is divided into two steps. Firstly, apply standard DT SI techniques [7], [11] to uniquely identify a model P_d. Secondly, reconstruct P_c from P_d. A necessary condition for reconstructing P_c uniquely from P_d is that the eigenvalues $\lambda_i(A_c^p)$ can be determined uniquely from $\lambda_i(A_d^p)$, $i = 1, \ldots, n_x$. The mapping of these eigenvalues follows from Lemma 5 and is given by

$$\lambda_i(A_d^p) = e^{\lambda_i(A_c^p)h} = e^{\sigma_i h} e^{j\omega_i h}, \quad (7)$$

which is definitely not an injection due to periodicity with period $\frac{2\pi}{h}$. A sufficient condition for the unique computation of $\lambda_i(A_c^p)$ is thus

$$|\omega_i| < \frac{\pi}{h}, \ i = 1, \ldots, n_x. \quad (8)$$

Condition (8) is not satisfied in general since the location of the eigenvalues of P_c is unknown. ■

C. Modeling for SD control

From Proposition 4, it is clear that the model resulting from SI operates at the same sampling frequency as the data upon which the model is based. SD control requires a CT model of the plant. Hence, it is not possible to combine SD control with SI. Thus, if the model does not represent intersample behavior, it is not possible to design for good intersample behavior. Proposition 4 also obstructs the usage of first principles models in conjunction with parameter estimation methods due to non-unique parametrizations.

One approach to combine SI with the benefits of direct SD control is to identify the plant at a faster sampling frequency than the frequency at which the high-performance controller will be operating. Indeed, in high-performance feedback control, a significant amount of time is required to compute a new controller input in between two sampling instants. This lower bound on the sampling time is not present for SI, which can be performed off-line. For instance, data can be extracted from the plant at a higher sampling frequency by temporarily implementing a low-complexity controller that requires less computational time and hence can be implemented with a higher sampling frequency.

In Section III, a design framework is presented that enables the design of a DT controller resulting in satisfactory intersample behavior. Thereto, two plant models are used:

- P_d, operating at a low sampling frequency ω_s at which the resulting high-performance controller will operate,
- $P_{d,h}$, operating at the highest possible sampling frequency $\omega_{s,h} = \frac{2\pi}{h_h} > \omega_s$ within physical limitations.

D. Problem formulation

In virtue of the above observations, the following issues are addressed in this paper.

Q1. How should aliased resonance phenomena be handled during control design, *i.e.*, if poles are located in the complementary frequency bands $\frac{\omega_s}{2} < |\omega| < \frac{\omega_{s,h}}{2}$ of $P_{d,h}$ and aliasing occurs when downsampling $P_{d,h}$ to P_d?

Q2. Is there a problem if $P_{d,h}$ contains aliased dynamics?

Q3. Modeling of $P_{d,h}$ is performed over a larger frequency range and resonance dynamics may be less densely spaced than in case of P_d. Is it then possible to model P_d more accurately by first modeling $P_{d,h}$ and then downsampling that model instead of modeling P_d directly?

These issues are addressed in the remainder of this paper. First, the control design philosophy for high-performance SD systems is discussed.

III. DESIGN FRAMEWORK FOR SD CONTROL

In Section II-C, it is motivated that SI techniques cannot be combined straightforwardly with direct SD control due to modeling limitations. The best feasible approximate in the sense of modeling limitations is an MR solution, where the model $P_{d,h}$ is used to design for good intersample response. In this section, a practically feasible control design approach in the MR framework is discussed. This background is required for the results in Section IV and V.

A key issue in the design for MR and SD systems is the fact that such systems are linear periodically time varying (LPTV) [2], [3]. The main reason is that both $\mathcal{S}$ and $\mathcal{H}$ are linear, but (periodically) time varying operators. This has a severe implication for control system design: the frequency separation principle does not hold. This implies that standard control design techniques, such as loopshaping and pole placement, cannot be applied directly. To facilitate the derivations in the MR framework, it is assumed that

$$\omega_{s,h} = F\omega_s, \ F = 2, 3, \ldots. \quad (9)$$

To properly handle the LPTV aspect in MR control system design, an iterative control design cycle is proposed [9], [10]:

Step 1. Design a controller in an LTI framework. Dispose of the intersample behavior information from the model by downsampling $P_{d,h}$ to P_d. The feedback interconnection of P_d and K_d is DT and LTI. Next, design a controller using any DT synthesis technique, *e.g.*, using DT $\mathcal{H}_\infty$ loopshaping.

Step 2. Evaluate the intersample response in an MR analysis using the MR frequency domain tools in [10]. Clear guidelines enable the iterative improvement of the control design in Step 1 if the intersample response is not satisfactory.

Concluding, if both the modeling limitations and LPTV design aspects are considered in the control design for high-performance SD systems, then a DT control design for the model P_d arises at some point during the design procedure. This model can contain aliased effects, see Question Q1 in Section II-D, which is discussed in Section V.

IV. SYSTEM DOWNSAMPLING

In this Section, Question Q3 in Section II-D is addressed. First, a lemma is stated in Section IV-A that enables the downsampling of system models. In Section IV-B, the experimental setup is introduced and Lemma 6 is applied.

A. Theory

The following lemma enables the computation of a downsampled system. The idea is that an MR equivalent of the SD ZOH interpolator $\mathcal{H}$ holds the input to the plant $P_{d,h}$ for F samples. The fast sampled plant output is downsampled by an MR equivalent of the sampler $\mathcal{S}$.

Lemma 6 *Let a model $P_{d,h}$ of the system with sampling frequency $\omega_{s,h}$ be given by*

$$P_d^h = \left[\begin{array}{c|c} A_{d,h}^p & B_{d,h}^p \\ \hline C_{d,h}^p & D_{d,h}^p \end{array}\right]. \tag{10}$$

Then a state-space realization of the downsampled system P_d, see Fig. 1 and (6)*, is given by*

$$\begin{bmatrix} A_d^p & B_d^p \\ \star & \star \end{bmatrix} = \begin{bmatrix} A_{d,h}^p & B_{d,h}^p \\ 0 & I \end{bmatrix}^F, \quad \begin{bmatrix} C_d^p \\ D_d^p \end{bmatrix} = \begin{bmatrix} C_{d,h}^p \\ D_{d,h}^p \end{bmatrix}, \tag{11}$$

where $\star$ denotes a matrix entry that is not used in further computations and F is defined in (9)*.*

Proof: Follows directly from successive substitution of the state equation $\xi_h[k+1] = A_{d,h}^p \xi_h[k] + B_{d,h}^p \nu_h[k]$ and $\nu_h[k+f] = \nu[\frac{k}{F}]$, $f = 0, \ldots, F-1$. ■

From (11) it is deduced that aliasing also arises in system downsampling. In particular, for computing P_d from P_c, it does not matter whether P_d is computed directly using Lemma 5 or by first computing $P_{d,h}$ using Lemma 5 and subsequent downsampling of $P_{d,h}$ to P_d using Lemma 6.

B. Experimental results

In this section, Lemma 6 is applied to an identified plant model at a high sampling frequency $\omega_{s,h}$. The hypothesis is that this enables a more accurate identification of flexible dynamics at the lower sampling frequency ω_s than direct identification with sampling frequency ω_s, since a larger frequency range is available during identification.

The experimental setup is a prototype wafer stage as described in Section I. The wafer stage is actuated and sensed in all six motion DOFs, see Fig. 2. Laser interferometers with sub-nanometer accuracy are used for sensing. By appropriate sensor and actuator transformations, the different DOFs are rigid-body decoupled. Only the z-direction is considered in identification, the other directions are controlled by low-bandwidth PID controllers to avoid interaction.

A high-performance feedback controller can be implemented with a maximum sampling frequency of $f_s = 1$ kHz. However, with a low bandwidth controller, the feedback loop can operate with sampling frequencies up to $f_{s,h} = 5$ kHz. This implies that $F = 5$ in (9). To illustrate the downsampling techniques, the plant frequency response function (FRF) is identified at both the sampling frequencies

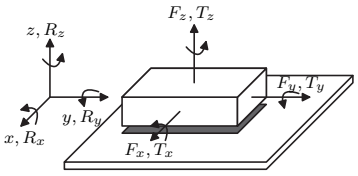

Fig. 2. Schematic illustration of a wafer stage.

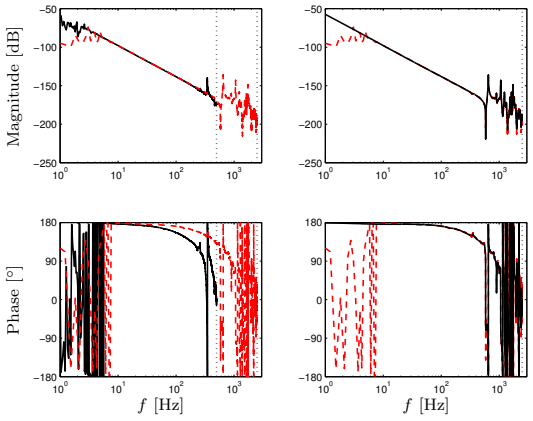

Fig. 3. Left: identified FRFs at $f_s = 1$ kHz (solid) and $f_{s,h} = 5$ kHz (dashed). Right: 60^{th} plant model $P_{d,h}$ (solid) and identified FRF (dashed), both at $f_{s,h} = 5$ kHz.

of $f_s = 1$ kHz and $f_{s,h} = 5$ kHz, see Fig. 3 for a Bode diagram. Note the appearance of aliasing in the plant FRF. In particular, in the $f_{s,h} = 5$ kHz FRF there is a resonance frequency at 653 Hz, which appears as an *aliasing* component at 347 Hz in the $f_s = 1$ kHz FRF.

A model is computed using DT curve-fitting techniques, see [11]. To obtain an accurate fit, a 60^{th} order model is selected. The results are depicted in Fig. 3. From visual inspection, the model fits the estimated FRF accurately.

Lemma 6 is applied to the 60^{th} order model operating with a sampling frequency of $f_{s,h} = 5$ kHz, see Fig. 4 for a Bode magnitude plot of the resulting model. The downsampled model has a resonance peak around 347 Hz, which is also present in the identified FRF at $f_s = 1$ kHz yet not in the model $P_{d,h}$ at 347 Hz. Hence, downsampling aliases high frequent dynamics, as is expected in Section IV-A.

The results in Fig. 4 confirm that identifying a plant at a high sampling frequency and subsequent downsampling is a sensible approach to obtain an accurate plant model at a lower sampling frequency. The main argument is the fact that resonance frequencies are less densely spaced that facilitates modeling procedures such as frequency response fitting.

Though the results in Fig. 4 are promising, an unexplained phenomenon arises in the downsampling procedure. If the downsampled model in Fig. 4 is investigated in detail, there is a significant mismatch in the aliased resonance dynamics around 347 Hz between the model and the identified FRF, both in frequency and magnitude, while the original model at 5 kHz has a significantly higher accuracy. One possible explanation for the mismatch in magnitude is the fact that the true system is nonlinear and the experiment was performed with a different excitation signal, *i.e.*, the frequency content of a ZOH reconstructed signal depends upon the sampling

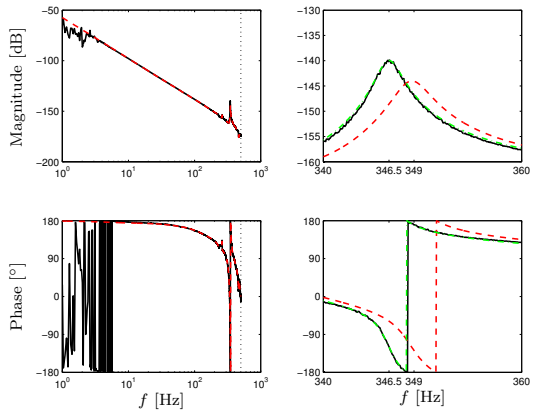

Fig. 4. Left: identified FRF (solid) and downsampled model of Fig. 3, both at $f_s = 1$ kHz. Right: detail figure of the left side, additionally, a 10^{th} order model is shown that is used for control design (dash-dotted).

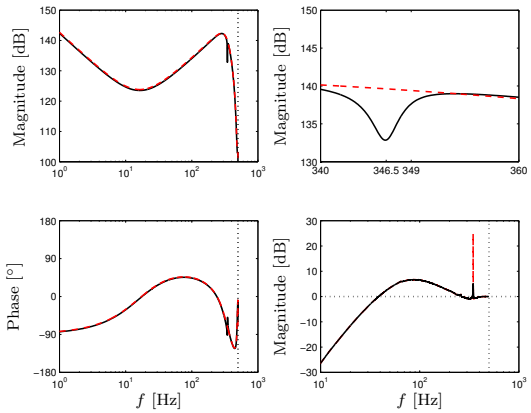

Fig. 5. Left: Bode diagram of Controller 1 (solid) and Controller 2 (dashed). Top right: detail of top left plot. Bottom right: Bode magnitude plot of $S_d(e^{j\omega h})$ using Controller 1 (solid) and Controller 2 (dashed).

frequency, see (5). Similar results have been obtained in a comparison between open-loop and closed-loop experimentation, see [13]. Additionally, the sampler $\mathcal{S}$ and reconstructor $\mathcal{H}$ may not be ideal as in Definitions 2 and 3. An LTI anti-aliasing filter could not have caused the discrepancy since from an identification perspective the anti-aliasing filter is part of the CT dynamics of the plant P_c.

V. SUPPRESSION OF ALIASED MODES

In this section, the control design for systems with aliased resonance phenomena is considered, *i.e.*, Questions Q1 and Q2 in Section II-D are addressed. In Section V-A, a theoretical discussion on this issue is given that is illustrated by experimental results in Section V-B.

A. Theory

The first step is to show that if K_d stabilizes P_d, then it also stabilizes the underlying faster DT model $P_{d,h}$ and the underlying CT plant P_c of Assumption 1. This requires that stabilizability and detectability are preserved by sampling.

Lemma 7 *If Assumption 1 is satisfied, then there exists a controller K_d that stabilizes P_c, see Fig. 1, for all $\omega_s > 0$.*

Proof: See [10]. ■

Using the result in Lemma 7, it is now straightforward to show, *e.g.*, by integrating the CT differential equations, that if K_d internally stabilizes P_d, then it also stabilizes the underlying CT plant P_c and all plant models operating at a higher sampling frequency $f_{s,h}$.

Thus, standard DT tools can be applied to the feedback interconnection of P_d and K_d for analyzing *stability*. Indeed, it does not matter whether P_d contains aliased dynamics.

For analyzing *performance*, the DT model P_d can be used to compute the *at* sample response. In particular, DT closed-loop transfer functions, possibly containing aliased dynamics, give exact mappings between signals *at* the controller sampling instants. However, there are no guarantees that the resulting intersample response is satisfactory. To evaluate the intersample response, a time domain or frequency domain analysis can be performed, which requires a model $P_{d,h}$ operating at a sampling frequency $f_{s,h}$, see also Section III.

B. Experimental results

In this section, a controller is designed for a plant model that contains control-relevant aliased dynamics. The experimental setup is already described in Section IV-B. Due to the discrepancy between the downsampled model and the identified FRF in Fig. 4, the curve fitting algorithm is also applied to the identified FRF at $f_s = 1$ kHz. This model is of order 10 and is also depicted in Fig. 4 (right hand side).

A DT $\mathcal{H}_\infty$-loopshaping design is made using the approach proposed in [9] and weighting filters as suggested in [17]. The resulting controller is called Controller 1 and is of the proportional-integral-derivative (PID) type, with a bandwidth of approximately 65 Hz and a local low gain around 347 Hz, see Fig. 5. The exact $\mathcal{H}_\infty$-optimal control design is not important here since it resembles manual designs [14].

The optimal controller has a low gain exactly at the frequency of the aliased resonance peak at 347 Hz. From a CT perspective, there are no resonance dynamics at 347 Hz, see Fig. 3, and there is no reason to reduce the controller gain at this frequency. To illustrate the effect of not suppressing the aliased dynamics, the local low gain is removed using an *ad hoc* model reduction technique. The resulting controller is called Controller 2 and is depicted in Fig. 5.

Controller 2 results in a large peak in the Bode magnitude plot of the DT sensitivity function $S_d = (I + P_d K_d)^{-1}$, see Fig. 5. This implies poor disturbance rejection properties at the frequency of 347 Hz. This is confirmed by the experimental results in Fig. 6, where both Controller 1 and 2 are implemented. No reference signals are applied, the system is excited by external disturbances. The 1 kHz measurement shows that the response is satisfactory for Controller 1, whereas Controller 2 results in a relatively large error. In particular, Controller 2 results in a dominant 347 Hz component, see the cumulative power spectral density (CPS). Concluding, regarding the *at* sample response, aliased resonance phenomena should be suppressed.

The intersample response has not yet been addressed in the discussion. In particular, suppressing the aliased resonance *at* the controller sampling instants could deteriorate the response *in between* the controller sampling instants.

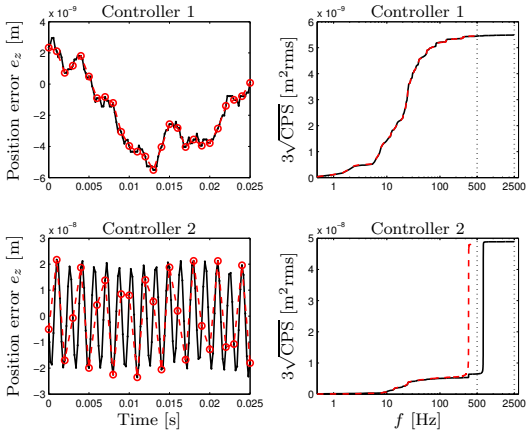

Fig. 6. Measured stand-still errors, measured at $f_{s,h} = 5$ kHz (solid), measured at $f_s = 1$ kHz (dashed). Note the different scaling of the axes.

However, in Fig. 6 it is clear that suppressing aliased resonance phenomena *at* the controller sampling instants, *i.e.*, the response using Controller 1, does not deteriorate the intersample response. Additionally, it is interesting to consider the intersample response using Controller 2: the true error signal does not contain a 347 Hz dominant frequency, but a 653 Hz dominant frequency component.

Concluding, both from an SD and DT perspective no distinction should be made for aliased plant dynamics when designing a DT controller K_d for the plant P_d, *i.e.*, Step 1 in Section III. Furthermore, a CT control design approach with *a posteriori* discretization is inferior to a DT approach, *i.e.*, if the digital controller implementation is neglected an unsatisfactory control design similar to Controller 2 would have been obtained.

The above intersample results are supported by the MR frequency domain analysis tools as presented in [10], see also Section III. However, this is beyond the scope of this paper. The MR tools also provide insight in the reason for the satisfactory intersample response. The key issue is that a low control gain results in a low control sensitivity $K_d S_d$ that is an indicator for good intersample response to aliased phenomena [10].

VI. CONCLUSIONS

In this paper, the aliasing of plant dynamics in SD control systems has been investigated. The main results are as follows, see also Section II-D.

A1. From an *at*-sample analysis, no distinction should be made for aliased dynamics during control design, *i.e.*, aliased dynamics should also be suppressed in a DT control design. The suppression of aliased dynamics is also required for achieving satisfactory intersample performance.

A2. If an MR intersample analysis is performed, the plant model $P_{d,h}$, operating at a higher sampling frequency $\omega_{s,h}$ than the controller sampling frequency ω_s, should contain all phenomena observed at that frequency, *i.e.*, including aliased effects. Then, the MR tools enable an exact analysis of the intersample response at the frequency $\omega_{s,h}$.

A3. A procedure for accurately identifying high-frequency dynamics is presented.

In addition, it is shown that a CT control design approach with *a posteriori* controller discretization is not capable of suppressing aliased plant dynamics and is from this perspective inferior to DT or SD control design.

An open issue related to Item A3 above is the large discrepancy (from a closed-loop relevant perspective) between the downsampled plant model and the identified FRF at that frequency. This implies that the downsampled model is not suitable for high-performance control design. Moreover, MR frequency domain analysis tools may give inaccurate results, since these are based on LTI assumptions. A possible explanation is that the true system is not LTI or the sampler and ZOH interpolator are not ideal. Investigation of the model quality is subject to further research. The model inaccuracy can be captured by an uncertainty model in addition to the nominal model. Downsampling of model uncertainty and its implications for the structure and size of the uncertainty model require further research.

REFERENCES

[1] K. J. Åström, P. Hagander, and J. Sternby. Zeros of sampled systems. *Automatica*, 20(1):31–38, 1984.

[2] B. Bamieh, J. B. Pearson, B. A. Francis, and A. Tannenbaum. A lifting technique for linear periodic systems with applications to sampled-data control. *Syst. Contr. Lett.*, 17(2):79–88, 1991.

[3] T. Chen and B. Francis. *Optimal Sampled-Data Control Systems*. Springer, London, UK, 1995.

[4] J. C. Doyle and G. Stein. Multivariable feedback design: Concepts for a classical/modern synthesis. *IEEE Trans. Automat. Contr.*, 26(1):4–16, 1981.

[5] G. F. Franklin, J. D. Powell, and M. Workman. *Digital Control of Dynamic Systems*. Addison Wesley Longman, Menlo Park, CA, third edition, 1998.

[6] P. C. Hughes. Space structure vibration modes: How many exist? which ones are important? *Contr. Syst. Mag.*, 7(1):22–28, 1987.

[7] L. Ljung. *System Identification: Theory for the User*. Prentice Hall, Upper Saddle River, NJ, second edition, 1999.

[8] C. A. Mack. The new, new limits of optical lithography. In *Proc. Emerging Lithographic Technologies*, volume 5374, pages 1–8, Santa Clara, CA, 2004.

[9] T. Oomen, M. van de Wal, and O. Bosgra. Exploiting $\mathcal{H}_\infty$ sampled-data control theory for high-precision electromechanical servo control design. In *Proc. Americ. Contr. Conf.*, pages 1086–1091, Minneapolis, MN, 2006.

[10] T. Oomen, M. van de Wal, and O. Bosgra. Design framework for high-performance optimal sampled-data control with application to a wafer stage. *Accepted for publication in Int. J. Contr.*, 2007.

[11] R. Pintelon and J. Schoukens. *System Identification: A Frequency Domain Approach*. IEEE Press, New York, NY, 2001.

[12] C. E. Shannon. Communication in the presence of noise. *Proc. IRE*, 37:10–21, 1949.

[13] R. S. Smith. Closed-loop identification of flexible structures: An experimental example. *J. Guid., Contr, Dyn.*, 21(3):435–440, 1998.

[14] M. Steinbuch and M. L. Norg. Advanced motion control: An industrial perspective. *Eur. J. Contr.*, 4(4):278–293, 1998.

[15] G. Stix. Toward "point one". *Scient. Americ.*, 272(2):72–77, 1995.

[16] P. P. Vaidyanathan. *Multirate Systems and Filter Banks*. Prentice Hall, Englewood Cliffs, NJ, 1993.

[17] M. van de Wal, G. van Baars, F. Sperling, and O. Bosgra. Multivariable $\mathcal{H}_\infty/\mu$ feedback control design for high-precision wafer stage motion. *Contr. Eng. Prac.*, 10(7):739–755, 2002.

[18] P. M. J. Van den Hof and R. J. P. Schrama. Identification and control - closed-loop issues. *Automatica*, 31(12):1751–1770, 1995.

[19] S. R. Weller and R. H. Middleton. On the role of sampling zeros in robust sampled-data control design. In *Proc. Conf. Dec. and Contr.*, pages 325–330, Tampa, FL, 1998.

[20] Y. Yamamoto. A function space approach to sampled data control systems and tracking problems. *IEEE Trans. Automat. Contr.*, 39(4):703–713, 1994.